Indian Journal of Chemical Technology
Vol. 33, March 2026, pp. 246-257
DOI: 10.56042/ijct.v33i2.21683

# Ultrasound-assisted process intensification for the synthesis of nitrogen-doped ZnO photocatalyst and its application to malachite green degradation

Sachin A. Dhakare[1], Dipak U. Giram[2], Ravindra G. Puri[3] & Rajkumar S. Sirsam[1]*

[1]Department of Chemical Engineering, Kavayitri Bahinabai Chaudhari North Maharashtra University, Jalgaon 425 001, Maharashtra, India

[2]Department of Chemical Engineering, Shri Guru Gobind Singhji Institute of Engineering and Technology (SGGSIE&T), Nanded, 431 606, Maharashtra, India

[3]Department of Paint Technology, Kavayitri Bahinabai Chaudhari North Maharashtra University, Jalgaon 425 001, Maharashtra, India

*E-mail:rajkumarsirsam@gmail.com

*Received 16 July 2025; accepted 13 February 2026*

This research study illustrates that synthesizing nitrogen-doped ZnO (N–ZnO) nanoparticles using ultrasound is a viable alternative method for improving photocatalytic performance. Acoustic cavitation during ultrasonication leads to improved incorporation of nitrogen atoms, a decrease in crystallite size, and alteration of the electronic structure of the N–ZnO nanoparticles, which ultimately improves their catalytic properties. The N–ZnO nanoparticles synthesized by this method have been extensively characterized using XRD, FESEM, EDS, XPS, and UV-visible spectroscopy. XRD analysis confirmed the hexagonal wurtzite structure of ZnO with successful nitrogen incorporation, which induced lattice distortions and reduced crystallite size. FESEM analysis revealed irregular and non-uniform morphology of the N–ZnO crystallites. Moreover, the successful and uniform incorporation of nitrogen ions into the crystal lattice of the ZnO particles is confirmed by both EDS and XPS analysis. Additionally, UV-Visible spectroscopy indicated a significant red shift in the absorption edge and a reduction in the bandgap from 3.21 eV (ZnO) to 2.59 eV (N-ZnO), enhancing visible-light absorption. Furthermore, the photocatalytic activity of N-ZnO has been evaluated for malachite green (MG) dye degradation under various operating conditions. Among the samples, 3% N-ZnO exhibited a maximum degradation efficiency of 96.43% at a photocatalyst loading of 0.15 g/100 mL of dye solution, an initial dye concentration of 20 ppm, and pH 12. Kinetic analysis demonstrated that MG degradation followed pseudo-first-order reaction kinetics. Thus, the results of this study support the use of ultrasound-assisted synthesis as an effective method for the preparation of N-ZnO nanoparticles.

**Keywords:** Dye degradation, Malachite green, Nitrogen-doped ZnO, Optimization, Photocatalyst, Ultrasound method

## Introduction

Rapid industrialization and urbanization over the past few decades have led to an increased discharge of synthetic dyes into water bodies, posing significant environmental and health challenges[1]. Malachite green (MG) is one of the most well-known synthetic dyes due to its extensive use in the textile, leather, and paper industries. Moreover, MG is known to be carcinogenic, mutagenic, and teratogenic, making its removal from wastewater a critical environmental concern[2]. Conventional water treatment methods often fall short of addressing these challenges effectively, necessitating the development of advanced and efficient technologies for dye degradation[3,4].

Photocatalysis has emerged as a promising solution for the degradation of dyes in water[5,6]. Zinc oxide (ZnO) is a widely studied photocatalyst due to its excellent photocatalytic properties, environmental friendliness, and cost-effectiveness[7,8]. However, pure ZnO has some limitations, including a wide bandgap (~3.37 eV) which restricts its photocatalytic activity to the UV region, accounting for only about 4% of the solar spectrum[9,10]. To enhance its photocatalytic performance under visible light, various strategies have been explored, among which doping with non-metals, such as nitrogen (N), has shown significant promise[11]. Nitrogen doping introduces new energy levels within the bandgap of ZnO, thereby narrowing the bandgap and extending the absorption edge into the visible region[12]. This modification improves the light-harvesting capability and enhances the separation efficiency of photogenerated electron-hole pairs, leading to increased photocatalytic activity. According to the literature, numerous studies have demonstrated the potential of N-doped ZnO (N-ZnO) in the degradation of various dyes, including Amaranth, Methyl Orange, Methylene Blue, Rhodamine 6G, and

Rhodamine B[8,13–19]. A detailed summary of these reported studies is provided in the Supplementary Information (Table S1). Although nitrogen-doped ZnO has been reported for the photocatalytic degradation of several organic dyes, its application toward malachite green degradation has not been previously published. Further, the synthesis method of the photocatalyst plays a crucial role in determining its structural and functional properties. Traditional methods, such as sol-gel, hydrothermal, and co-precipitation, are time-consuming and require high energy consumption[20]. Recently, ultrasound-assisted synthesis has gained attention due to its simplicity, efficiency, and ability to produce high-quality nanomaterials with desirable properties. Ultrasound irradiation generates acoustic cavitation, leading to high local temperatures and pressures, which enhance chemical reactivity and promote the formation of uniformly doped nanoparticles with a high surface area and improved photocatalytic properties[21,22].

Most earlier studies rely on conventional synthesis routes, which offer limited control over dopant incorporation and defect formation. In the present work, an ultrasound-assisted synthesis approach is employed as a process intensification strategy to prepare nitrogen-doped ZnO nanoparticles with varying weight percentages (1%, 3%, and 5%) and applied for the photocatalytic degradation of MG dye under sunlight. Additionally, this research focused on optimizing photocatalytic variables such as the type of photocatalyst, catalyst dosage, initial pH, and dye concentration using a one-parameter-at-a-time approach to enhance the efficiency of the degradation process. The synthesized N-ZnO nanoparticles were characterized using various analytical techniques to analyze their structural, optical, and photocatalytic properties. Furthermore, the dye degradation mechanism of MG has also been proposed. To the best of the authors knowledge, this is the first study reporting the ultrasound-assisted synthesis of nitrogen-doped ZnO and its application for the degradation of malachite green dye under sunlight. This work clearly shows how ultrasound-based process intensification improves material properties and enhances photocatalytic performance.

## Experimental Section

### Materials

The materials used in this study included analytical-grade zinc acetate dihydrate [$Zn(CH_3COO)_2 \cdot 2H_2O$, purity 98%], urea ($NH_2CONH_2$, purity 99%), and sodium hydroxide pellets (NaOH, purity 99%), which were procured from Merck, India. The MG dye was purchased from Sigma-Aldrich and used as a target pollutant in the photocatalytic degradation process. The detailed properties of the MG dye are summarized in Table 1[23]. All reagents were used as received, without further purification. The experiments were conducted using double-distilled water as the solvent.

### Ultrasound-assisted synthesis of ZnO nanoparticles

To synthesize pure ZnO nanoparticles, 0.1 mol of zinc acetate dihydrate was initially dissolved in 50 mL of double-distilled water. The solution was sonicated for 30 min to ensure complete dissolution of all components. Subsequently, a 2 M sodium hydroxide solution was added dropwise to the zinc acetate solution until the pH reached 7, leading to the formation of a white precipitate. The mixture was then sonicated for an additional 30 min. The precipitate was then washed with distilled water, filtered, and dried in a hot air oven at 100°C for six hours. The dried precipitate was further ground using a mortar and pestle. Finally, the nanoparticles were annealed in a muffle furnace at 500°C for two hours to obtain the desired final product of ZnO nanoparticles.

The same procedure was followed for nitrogen-doped ZnO nanoparticles, with urea added as a dopant in varying amounts (1, 3, and 5 wt%) during the initial synthesis stage. Fig. 1 shows a detailed schematic of the N-doped ZnO synthesis process.

### Photocatalytic degradation of MG dye

The photocatalytic batch experiments were carried out in a 250 mL conical flask under direct sunlight exposure to evaluate the photocatalytic activity of the synthesized N–ZnO nanoparticles for the degradation of MG dye. The experiments were performed during the month of May within a fixed daily time window (11:00 a.m. to 2:00 p.m.) under clear sky conditions to minimize variations in sunlight intensity. The average solar irradiance during the experiments was measured

Table 1 — Detailed properties of MG Dye

| Chemical Name | Malachite Green |
|---|---|
| Chemical Formula | $C_{23}H_{25}ClN_2$ |
| Molecular Weight | 364.92 g/mol |
| IUPAC Name | 4-[(4-dimethylaminophenyl)-phenyl-methyl]-N,N-dimethylaniline chloride |
| Structure | Triphenylmethane-based dye |
| Appearance | Green crystalline powder |
| Solubility | Soluble in water, ethanol, and acetone |
| Type of Dye | Cationic (Basic) Dye |
| Absorption ($\lambda_{max}$) | ~ 615–620 nm in aqueous solution |

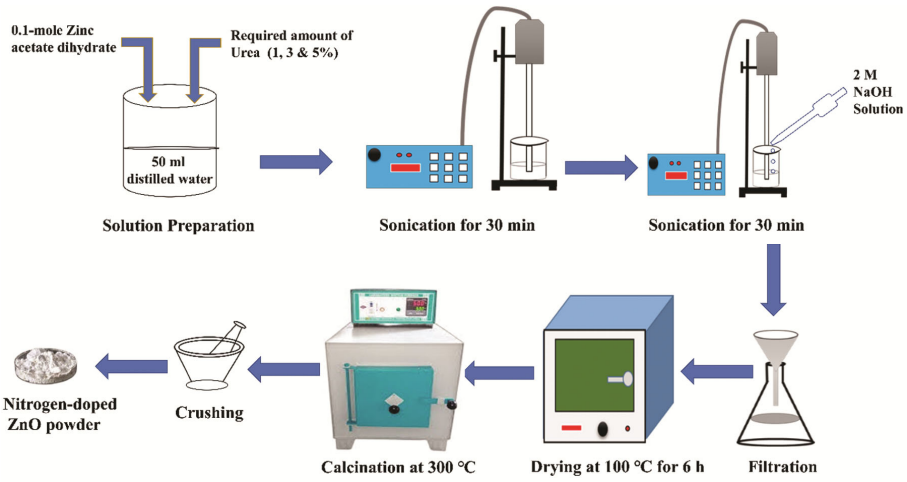


Fig. 1 — Schematic synthesis of N-ZnO (1, 3 and 5%) samples

(approximately 80000 to 100000 lux) using a lux meter and maintained at comparable levels for all runs. Initially, a specific quantity of N-ZnO nanoparticles was added to a 100 mL solution containing 20 ppm of the dye. This mixture was vigorously stirred in the absence of light for 30 min to establish adsorption-desorption equilibrium. Subsequently, 4 mL aliquots were extracted from the reaction mixture, and subjected to centrifugation at 5000 RPM, after which absorbance of the resulting supernatant was measured at a wavelength of 617 nm using a UV-Visible spectrophotometer to determine the concentration of MG dye. The percentage removal of MG dye was determined using the following equation[24]:

$$\% \text{ decolourization} = \left(1 - \frac{C}{C_0}\right) \times 100 \quad \ldots(1)$$

In this equation, $C_0$ and C represent the initial and final concentrations of MG dye, respectively. Similar experiments were conducted under varying conditions, including the type of photocatalyst (1,3 and 5% N-ZnO), catalyst loading (ranging from 0.05 g to 0.2 g per 100 mL dye solution), dye concentration (ranging from 10 ppm to 40 ppm), and pH levels (2, 7, and 12). The objective was to identify the optimal conditions that would yield the highest level of MG dye decolorization. All comparative photocatalytic experiments were conducted within the same daily time window and under similar solar irradiance conditions to ensure a fair comparison of photocatalytic performance among the samples.

### Characterization

The crystallographic characteristics of all synthesized nanoparticles were examined using X-ray diffraction analysis (Rigaku Mini-Flex X-ray diffractometer). The nanoparticle's surface morphology and elemental composition were analyzed using a Field Emission Scanning Electron Microscope (FESEM, Carl Zeiss, Germany) equipped with an energy-dispersive X-ray Spectroscopy (EDS) detector. The chemical states and elemental composition were identified using an XPS spectrophotometer (Thermo Fisher). Additionally, the UV-visible spectra of the samples were recorded using a Lab India UV-3200 spectrophotometer.

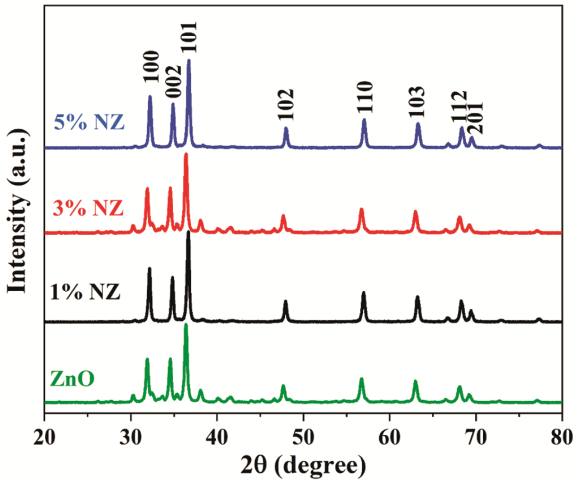


Fig. 2 — XRD pattern of ZnO and N-ZnO (1% NZ, 3% NZ, and 5% NZ) nanoparticles

## Results and Discussion

### Characterization of ZnO and Nitrogen-doped ZnO (N-ZnO) nanoparticles (1%, 3%, and 5%)

#### *XRD analysis*

Fig. 2 illustrates the XRD patterns of pure ZnO and nitrogen-doped ZnO nanoparticles (1%, 3%, and 5%).

The XRD patterns exhibit characteristic diffraction peaks at 2θ values of 31.88°, 34.46°°, 36.35°, 47.64°, 56.69°, 62.94°, 68.34°, and 69.04° corresponding to the (100), (002), (101), (102), (110), (103), (112), and (201) planes of the hexagonal wurtzite structure, respectively[25]. The XRD patterns of N-doped ZnO nanoparticles exhibit similar peak positions to those of pristine ZnO, indicating that the doping process does not significantly alter the primary crystal structure of ZnO. However, slight shifts in peak positions and variations in peak intensities confirm the incorporation of N ions into the ZnO lattice, which induces lattice distortion. Furthermore, the average crystallite sizes of the synthesized samples were calculated using the Debye–Scherrer equation[26]. The estimated crystallite sizes for ZnO, 1% NZ, 3% NZ, and 5% NZ were 19.62, 18.36, 17.67, and 16.92 nm, respectively. The crystallite size decreases from 19.62 nm (ZnO) to 16.92 nm (5% N–ZnO), which is beneficial for photocatalysis as smaller crystallites provide higher surface area and more active sites for dye degradation.

***FESEM and EDS analysis***

The morphological characteristics of ZnO and N-ZnO nanoparticles were analyzed using FESEM images, as shown in Fig. 3 (a, c, e, g). The incorporation of nitrogen did not result in significant changes to the overall morphology compared to pure ZnO nanoparticles. All samples exhibited irregular and non-uniform shapes. However, with increasing nitrogen content, further distortion in particle shape and random orientation of nanoparticles were observed. The average size of the ZnO nanoparticles was approximately 210±50 nm, while N-ZnO samples exhibited an average size of around 270±50 nm, consisting of smaller aggregated nanoparticles.

Furthermore, Fig. 3(b, d, f, h) presents the EDS spectra of undoped and N-ZnO nanostructures. The spectra confirm the presence of Zn, O, and N, verifying the successful incorporation of nitrogen into the ZnO matrix.The EDS is limited in its ability to accurately identify and measure light elements such as nitrogen, especially when they are present in low amounts. Therefore, the nitrogen detected by EDS is near its limit of detection and should only be considered as evidence of N incorporation in a qualitative sense. A comprehensive EDS analysis of ZnO and N-ZnO nanoparticles is provided in Table 2. Additionally, Fig. 4 depicts the EDS mapping of N-ZnO nanostructures, specifically for the 5%NZ sample, providing further evidence of the uniform distribution and successful nitrogen doping within the ZnO matrix.

***XPS analysis***

The XPS spectrum of N-ZnO (5%NZ) nanoparticles is shown in Fig. 5. The survey spectrum revealed peaks corresponding to Zn, O, and N, with no detectable impurities, indicating high sample purity. The Zn 2p peaks at ~1021.5 eV and ~1044.6 eV correspond to $Zn^{2+}$ in the ZnO lattice. The O 1s spectrum exhibited a dominant peak at ~530.2 eV, attributed to lattice oxygen, and a secondary peak at ~531.6 eV, corresponding to oxygen defects or surface-adsorbed species. Importantly, the N 1s spectrum displays a distinct peak at ~348.8 eV, which is characteristic of substitutional nitrogen (N–ZnO), confirming that nitrogen is incorporated into the ZnO lattice[27]. These results confirm the successful doping of nitrogen into ZnO, leading to potential modifications in the electronic structure and an enhancement in photocatalytic activity.

***UV-visible analysis***

The UV-visible absorption spectra of pure ZnO and N-ZnO were analyzed, as shown in Fig. 6. A significant redshift (Fig. 6a) in the absorption edge of N-ZnO photocatalysts was observed compared to pure ZnO, indicating a band gap reduction. This redshift is attributed to the introduction of localized energy states within the band gap due to the incorporation of N ions[28].

The optical band gap of the photocatalysts was calculated using the Tauc plot method. The Tauc plot analysis (Fig. 6b) revealed a decrease in the band gap from 3.21 eV for pure ZnO to approximately 2.59 eV for N-ZnO. This reduction in the band gap enhances the absorption of UV light, promoting the generation of electron-hole pairs and thereby improving the photocatalytic performance of the N-ZnO photocatalysts.

**Photocatalytic activity**

***Effect of photocatalyst***

The effect of different photocatalysts (ZnO, 1% NZ, 3% NZ, and 5% NZ) on MG dye degradation was evaluated, as shown in Fig. 7. The results revealed that nitrogen doping consistently enhanced degradation efficiency, though the extent of enhancement depended on the doping concentration. Increasing the doping concentration up to 3% significantly improved the removal efficiency, rising

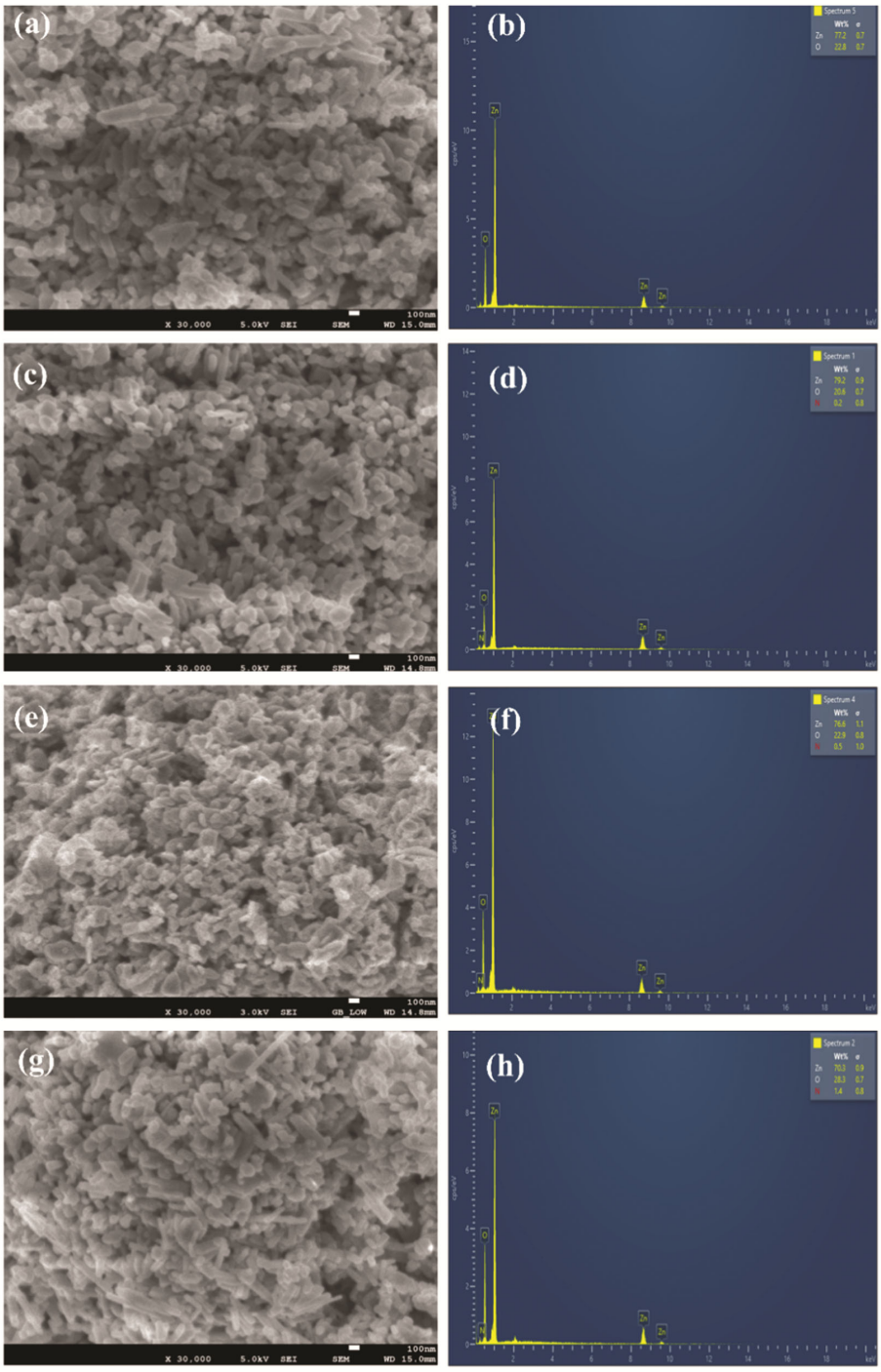


Fig. 3 — FESEM and EDS analysis of ZnO (a,b), 1% NZ (c,d), 3% NZ (e,f), and 5% NZ (g,h) nanoparticles

from 41.35% to 90.06%. The increase in degradation percentage may be due to the reduction in electron-hole recombination as doping of ZnO with nitrogen introduces a new energy level below the conduction band. However, a further increasing the concentration to 5% led to a slight reduction in removal efficiency to 81.56%. This might be due to the creation of excess oxygen vacancies which provide the recombination centers for the electrons and holes[29]. Based on these findings, 3% NZ was identified as the optimal photocatalyst for MG dye degradation.

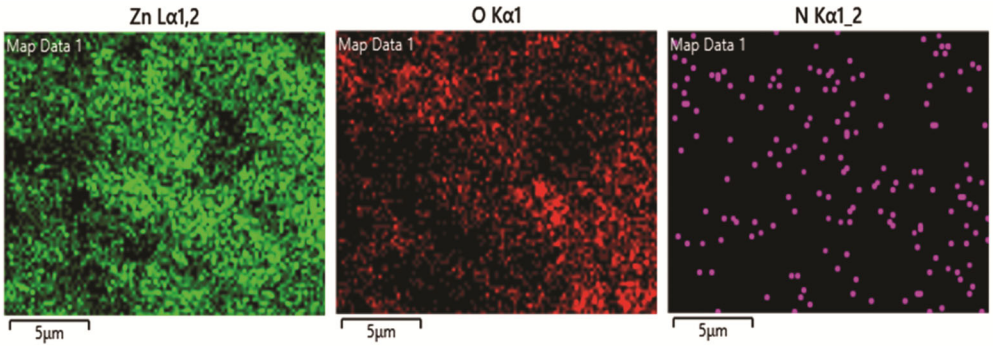


Fig. 4 — Elemental mapping of 5%NZ sample

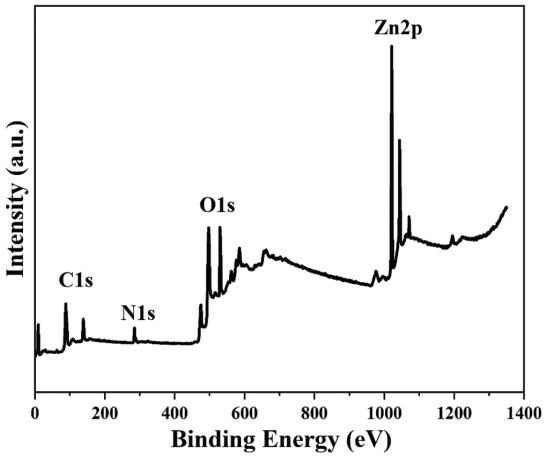


Fig. 5 — XPS spectrum of 5%NZ sample

Table 2 — Detailed EDS analysis of ZnO and N-ZnO samples

| Sample | Elements | Wt% |
|---|---|---|
| ZnO | Zn | 77.2 |
| | O | 22.8 |
| 1% NZ | Zn | 79.2 |
| | O | 20.6 |
| | N | 0.2 |
| 3% NZ | Zn | 76.6 |
| | O | 22.9 |
| | N | 0.5 |
| 5% NZ | Zn | 70.3 |
| | O | 28.3 |
| | N | 1.4 |

***Effect of catalyst loading***

Fig. 8 illustrates the influence of photocatalyst loading on MG dye degradation at an initial concentration of 20 ppm. The photocatalyst dosage was varied from 0.05 g to 0.2 g per 100 mL (0.5 to 2 g $L^{-1}$) dye solution to determine the optimal loading. Optimizing the dosage is critical for maximizing sunlight absorption, which is essential for effective MG dye degradation. However, excessive catalyst loading causes aggregate formation in the reaction medium, reducing photocatalytic efficiency under sunlight. The optimal photocatalyst dosage of 0.15 g achieved a maximum MG dye degradation of 90.72%. The degradation efficiency increased from 40.34% to 90.72% over 90 min as the catalyst dosage increased from 0.05 g to 0.15 g. This improvement is attributed to the higher number of active sites available at increased photocatalyst loadings, facilitating enhanced adsorption and degradation of MG dye. However, an increase in catalyst dosage to 0.2 g slightly reduced the degradation efficiency to 81.75%. This decline is attributed to photocatalyst particle aggregation at higher dosages, reducing the surface area available for photocatalytic reactions. Additionally, at higher dosages, the reaction mixture becomes opaque, hindering sunlight penetration and limiting photocatalyst activation, ultimately reducing its photocatalytic activity[30,31].

***Effect of initial dye concentration***

The influence of the initial concentration of MG dye on its degradation using a 3% NZ photocatalyst was investigated at varying concentrations of 10, 20, 30, and 40 ppm. The results, presented in Fig. 9, reveal that the percentage of MG dye degradation efficiency increased as the concentration rose from 10 ppm to 20 ppm. However, beyond 20 ppm, a decline in degradation efficiency was observed with further increases in dye concentration. Specifically, the highest degradation efficiency of 90.17% was recorded at 20 ppm, which then decreased to 80.06% at 40 ppm. This trend can be attributed to the reduced ratio of accessible active sites to the initial dye concentration at higher concentrations, which limits the degradation rate due to the insufficient availability of catalytic surface area[32].

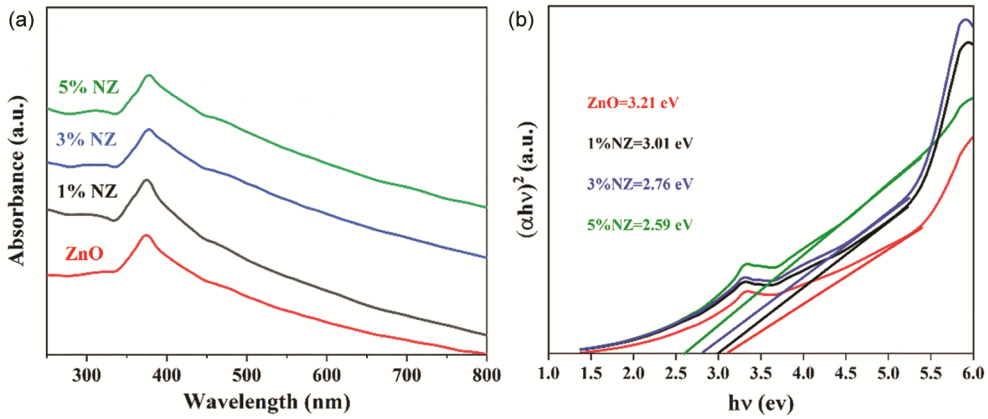


Fig. 6 — (a) UV-visible spectra (b) Tauc- plot of ZnO and N-ZnO nanoparticles

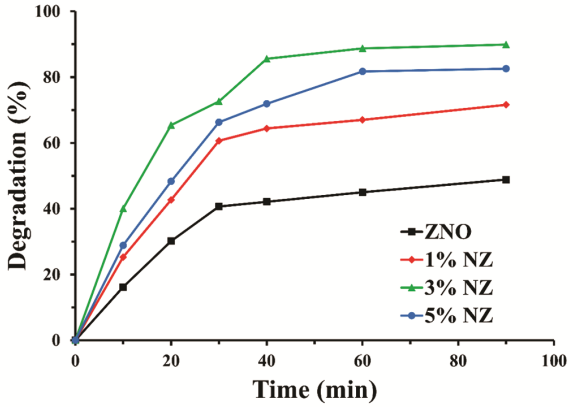


Fig. 7 — Effect of different photocatalyst (experimental conditions: photocatalyst loading 0.1 g, dye concentration 20 ppm, pH 7)

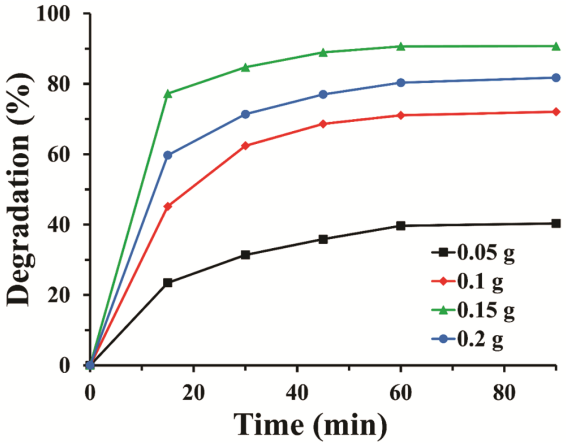


Fig. 8 — Effect of photocatalyst loading (experimental conditions: 3% NZ photocatalyst , dye concentration 20 ppm, pH 7)

***Effect of initial pH***

The effect of pH on the degradation of MG dye using N-ZnO photocatalyst is a critical parameter, as pH significantly impacts the surface charge of the photocatalyst. The degradation efficiency of MG dye

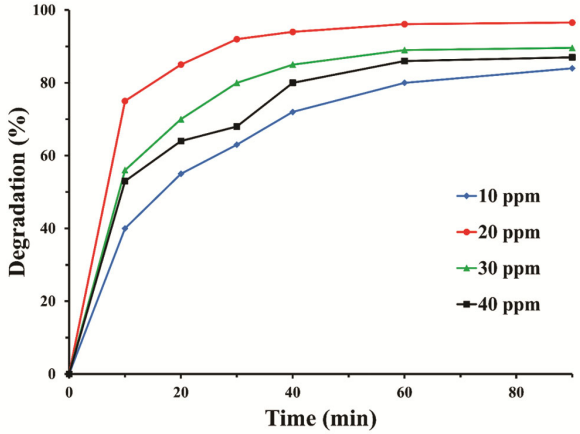


Fig. 9 — Effect of dye concentration (experimental conditions: 3% NZ photocatalyst, photocatalyst loading 0.15 g, pH 7)

was investigated at pH values of 2, 7, and 12, as illustrated in Fig. 10. These pH conditions were selected primarily for mechanistic understanding of the photocatalytic process. The results revealed that MG dye degradation was more efficient under basic conditions compared to acidic ones. At an acidic pH of 2, the degradation efficiency was recorded at 40.95%. This lower efficiency can be attributed to the protonation of the N-ZnO surface, leading to a positively charged surface. Since MG is a cationic dye, electrostatic repulsion between the dye molecules and the positively charged photocatalyst surface inhibits adsorption, consequently reducing degradation efficiency. Conversely, at higher pH values in the basic range, the surface of N-ZnO becomes negatively charged due to deprotonation. This negative surface charge facilitates the adsorption of MG dye molecules through electrostatic attraction, significantly enhancing degradation efficiency. Moreover, the basic environment promotes the generation of hydroxyl radicals (•OH),

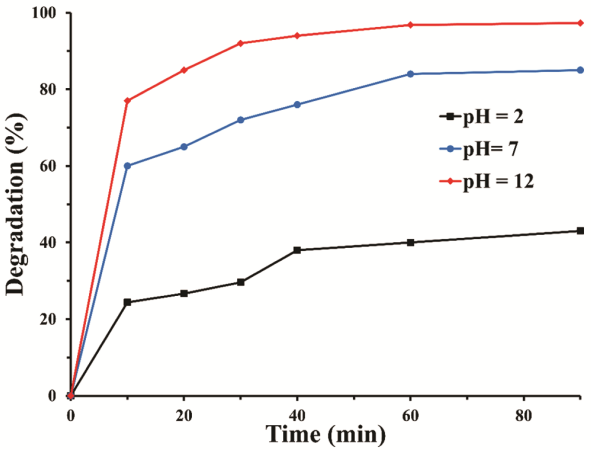


Fig. 10 — Effect of pH (experimental conditions: 3% NZ photocatalyst , photocatalyst loading 0.15 g, dye concentration 20 ppm)

which are highly reactive species crucial for the breakdown of dye molecules. The highest degradation efficiency of 96.43% was observed at a basic pH of 12, highlighting the favourable role of alkaline conditions in photocatalytic dye degradation[29]. Although alkaline pH enhances photocatalytic activity, operating under strongly alkaline conditions is not considered economically viable or environmentally sustainable for large-scale wastewater treatment due to the additional chemical consumption required for pH adjustment.

***Effect of different processes***

Fig. 11 shows the effect of different processes on the degradation of MG dye, which was investigated at optimized conditions. The experiments were conducted with a photocatalyst loading of 0.15 g, an initial dye concentration of 20 ppm, and a pH of 12. Among the processes studied, photolysis alone resulted in negligible dye degradation, indicating the limited ability of light irradiation to degrade MG dye in the absence of a photocatalyst. In contrast, ZnO photocatalysis demonstrated a significant improvement in degradation efficiency due to the generation of reactive oxygen species under light irradiation. However, the highest degradation efficiency was achieved using 3% N-ZnO as the photocatalyst, which exhibited superior activity due to its enhanced light absorption, improved charge separation, and increased generation of hydroxyl radicals (•OH) in the alkaline medium. This highlights the synergistic role of nitrogen doping in improving the photocatalytic performance of ZnO for MG dye degradation

Additionally, the time-dependent UV-visible spectra of MG dye were studied under optimized

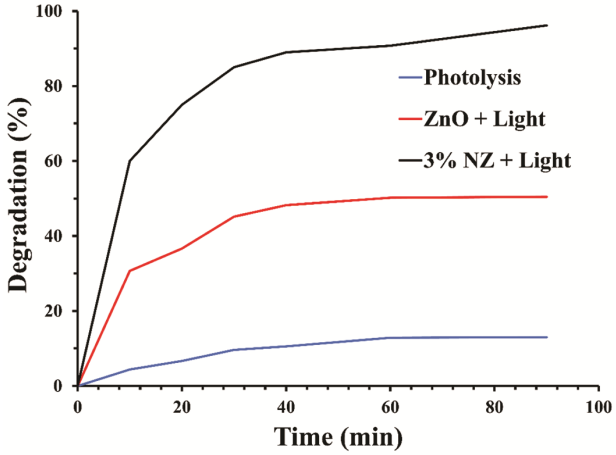


Fig. 11 — Effect of different processes (experimental conditions: 3% NZ photocatalyst, photocatalyst loading 0.15 g, dye concentration 20 ppm, pH 12)

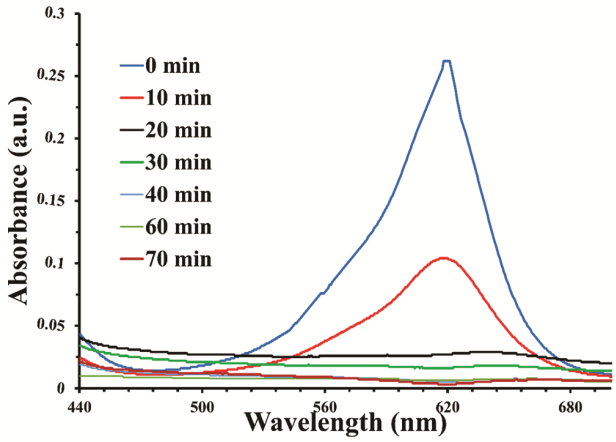


Fig. 12 — Time-dependent UV spectra at optimized conditions (experimental conditions: 3% NZ photocatalyst, photocatalyst loading 0.15 g, dye concentration 20 ppm and pH 12)

conditions using the 3% N-ZnO photocatalyst (Fig. 12). The spectra were recorded at regular time intervals to monitor the decrease in the characteristic absorption peak of MG dye, typically observed at around 617 nm. At the beginning of the reaction, the peak was sharp and intense, indicating a high concentration of MG dye in the solution. Over time, with the application of the 3% N-ZnO photocatalyst under light irradiation, the peak gradually decreased as the dye molecules were decomposed.

**Kinetic study of different photocatalysts at optimized conditions**

The degradation kinetics of MG dye were examined for pure ZnO and N-ZnO catalysts under their respective optimum reaction conditions

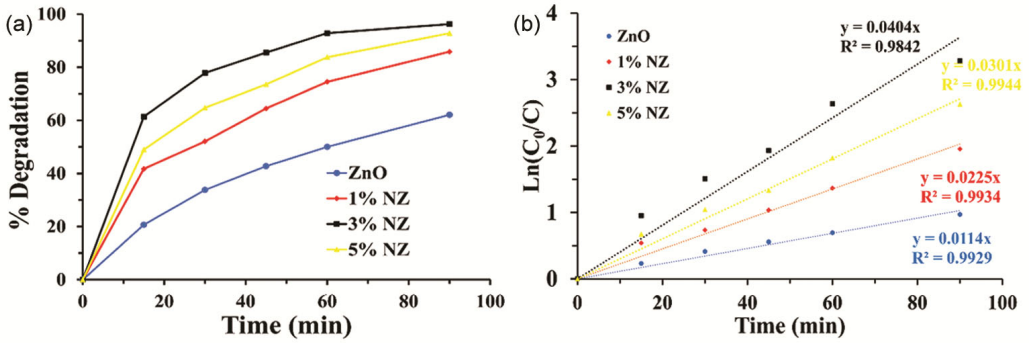


Fig. 13 — (a) Effect of different photocatalysts on MG dye degradation and (b) pseudo-first-order kinetic plots (ln C₀/C vs. time) under optimized conditions (3% N–ZnO photocatalyst, catalyst loading: 0.15 g, dye concentration: 20 ppm, pH 12)

Table 3 — Pseudo-first-order kinetic parameters for MG dye degradation over ZnO and N-ZnO photocatalysts

| Photocatalyst | Linear fit Equation | Rate Constant *(k)* | $R^2$ Value | Relative Kinetic Performance |
|---|---|---|---|---|
| Pure ZnO | y = 0.0114 x | 0.0114 | 0.9929 | Lowest |
| 1% NZ | y = 0.0225 x | 0.0225 | 0.9934 | Moderate |
| 3% NZ | y = 0.0404 x | 0.0404 | 0.9842 | Highest |
| 5% NZ | y = 0.0301x | 0.0301 | 0.9944 | Lower than 3% NZ |

(photocatalyst loading 0.15 g, dye concentration 20 ppm and pH 12), as shown in Fig. 13(b). The pseudo-first-order kinetic model, which is frequently used for heterogeneous photocatalytic reactions at low dye concentrations, was used to examine the kinetic data. This pseudo-first-order kinetic model is expressed as follows[7]:

$$ln\left(\frac{C_0}{C}\right) = kt \quad \ldots(2)$$

Where *'t'* is the irradiation period, *'k'* is the pseudo-first-order rate constant ($min^{-1}$), and '$C_0$' and 'C' are the initial and instantaneous dye concentrations, respectively.

The linear $ln(C_0/C)$ versus time*(t)* plots shown in Fig. 13(b) indicate that all catalysts degrade MG dye according to pseudo-first-order kinetics. Pure ZnO has the lowest slope, so it has the lowest k, indicating that it has relatively poor kinetics for degrading MG. On the other hand, as we increase the doping amount of nitrogen in N-ZnO from 1% to 3%, the slope of the linear plot becomes steeper with increasing '*k*', indicating accelerated kinetics. However, the 5% N-ZnO sample has a smaller slope than the 3% N-ZnO catalyst, indicating that severe nitrogen doping may result in recombination centers that prevent charge separation. The calculated rate constants, summarized in Table 3, clearly follow the order 3% N–ZnO > 5% N–ZnO > 1% N–ZnO > ZnO.

**Mechanism**

The degradation of MG dye using N-ZnO photocatalyst occurs through a photocatalytic mechanism driven by light irradiation (shown in Fig. 14). When exposed to light, N-ZnO absorbs photons, promoting electrons ($e^-$) from the valence band to the conduction band and creating electron-hole pairs ($e^-/h^+$). Nitrogen doping reduces the bandgap of ZnO, improving its visible-light absorption and extending its photocatalytic activity. The photogenerated holes ($h^+$) in the valence band react with water to form hydroxyl radicals ($OH^•$). Simultaneously, the electrons ($e^-$) in the conduction band reduce dissolved oxygen molecules to form superoxide radicals ($O_2^{-•}$). These reactive oxygen species ($OH^•$and $O_2^{-•}$) attack the MG dye molecules, breaking their chromophoric structures and ultimately leading to the mineralization of the dye into simpler, non-toxic compounds like $CO_2$ and $H_2O$. The enhanced charge separation and reduced recombination of $e^-/h^+$pairs due to nitrogen doping play a critical role in improving the efficiency of MG dye degradation[33].

**Radical scavenger study**

Experiments involving radical scavengers were conducted to examine the principal reactive species involved in photocatalytic degradation using 3% N-ZnO nanoparticles, as illustrated in Fig. 15. The photocatalyst demonstrated a high degradation efficiency (96.43%) when no scavenger was present. To evaluate how

individual radicals affect photocatalytic degradation, isopropyl alcohol (IPA) and benzoquinone (BQ) were added to the reaction system as scavengers for hydroxyl radicals ($OH^{\bullet}$) and superoxide radicals ($O_2^{\bullet-}$), respectively. Upon introducing IPA into the reaction mixture, the degradation efficiency decreased significantly, clearly showing that hydroxyl radicals are the primary reactive species contributing to the degradation process. In contrast, the introduction of BQ also reduced the degradation efficiency significantly, indicating the contribution of superoxide radicals. While both IPA and BQ reduced the degradation efficiency significantly, the reduction caused by IPA was greater than that caused by BQ; therefore, it can be concluded that the dominant radical species are $OH^{\bullet}$ radicals and the secondary species are $O_2^{\bullet-}$ radicals. Overall, the radical scavenger experiments confirm that the enhanced photocatalytic activity of 3% N-ZnO nanoparticles was mainly attributed to the presence of hydroxyl radicals with some contribution from superoxide radicals.

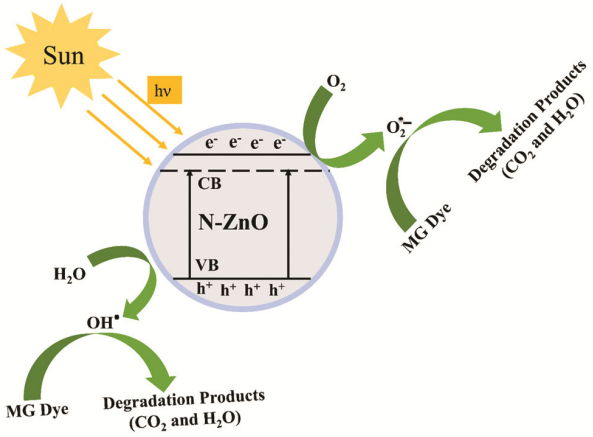


Fig. 14 — Proposed Mechanism of MG Dye Degradation by N-ZnO

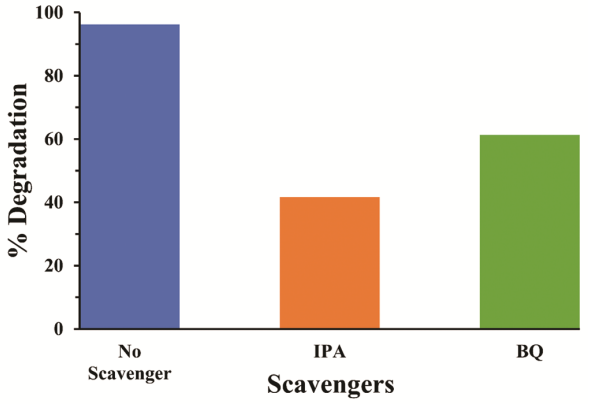


Fig. 15 — Radical scavenger study for MG dye degradation using 3% N–ZnO photocatalyst

**Reusability and stability**

To evaluate the recyclability and long-term stability of the synthesized 3%NZ photocatalyst, a cyclic degradation experiment was conducted under solar irradiation.The degradation efficiency of MG dye using the 3%NZ photocatalyst was systematically monitored over four cycles, with the corresponding results depicted in Fig. 16(a). Following each degradation cycle, the photocatalyst was recovered through centrifugation to ensure minimal loss of active material. To eliminate any residual organic contaminants, the recovered photocatalyst underwent a thorough washing, involving sequential rinsing with acetone and deionized water three times. Subsequently, the washed photocatalyst was subjected to drying at 90°C for 2 h to remove any adsorbed moisture and volatile components. The regenerated photocatalyst was then reused in subsequent degradation cycles under identical experimental conditions to assess its performance over repeated

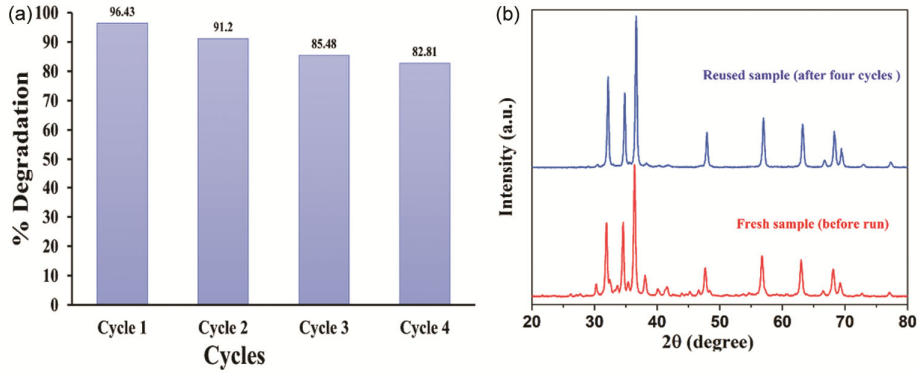


Fig. 16 — (a) Reusability and stability of 3% N–ZnO photocatalyst for MG dye degradation over four cycles and (b) XRD patterns of fresh and reused photocatalyst

applications. The recorded MG degradation efficiencies over four successive cycles were 96.43%, 91.2%, 85.48%, and 82.81%, respectively. Further, the XRD analysis of the photocatalyst used for photocatalytic reaction revealed no changes to the ZnO crystal structure when compared to the fresh sample, demonstrating excellent structural stability during the multiple photocatalytic use of the catalyst as shown in Fig. 16(b). A progressive decline in degradation efficiency was observed with increasing cycles, which can be attributed to several factors. Primarily, the adsorption of organic intermediates and degradation by-products on the photocatalyst surface can partially deactivate active sites, thereby reducing its overall photocatalytic activity. Additionally, minor losses of the photocatalyst during the recovery and washing processes could contribute to the observed decrease in efficiency. Furthermore, prolonged exposure to reaction conditions may induce structural or morphological changes in the photocatalyst, affecting its reusability. The lack of post-reaction SEM and XPS analysis is a limitation of this study and will be considered in future investigations.

#### Chemical Oxygen Demand analysis

Chemical oxygen demand (COD) analysis was performed utilizing 3% N–ZnO photocatalyst under the optimized photocatalytic conditions to assess the total amount of oxidizable organic material in a treated MG dye solution. COD of the MG dye solution prior to and after degradation has been estimated. The initial COD of the dye contaminant was found to be 245 mg/L, while the final COD after degradation was 48 mg/L, which reflects a COD reduction of approximately 80.40%. This significant decrease in COD values after photocatalysis supports the conclusion that the chromophoric molecules of the MG dye not only underwent decolourization but also partially oxidized to form smaller and simpler molecules.

## Conclusion

In this study, pure ZnO and nitrogen-doped ZnO (N-ZnO) photocatalysts were successfully synthesized using an ultrasound-assisted method and exhibited exceptional performance in the degradation of MG dye. XRD analysis confirmed the retention of the hexagonal wurtzite structure of ZnO with nitrogen doping, accompanied by a reduction in crystallite size, enhancing surface area and active sites for photocatalytic reactions. FESEM and EDS analyses demonstrated consistent morphology and successful nitrogen incorporation, while XPS analysis confirmed the substitutional doping of nitrogen into the ZnO lattice, contributing to modifications in the electronic structure. UV-Visible spectroscopy and Tauc plot analysis revealed a significant red shift and bandgap reduction, enabling better light absorption in the visible range. Photocatalytic experiments showed that N-ZnO nanoparticles, particularly at 3% doping, achieved a maximum degradation of 96.43%, due to improved charge separation, enhanced hydroxyl radical generation, and favourable adsorption characteristics under basic conditions (pH 12). Furthermore, kinetic analyses demonstrated that MG dye degradation followed a pseudo-first-order reaction model. Radical scavenger tests revealed that hydroxyl radicals were the primary reactive species, with superoxide radicals playing a minor role in the breakdown process. In addition, COD measurement revealed a large reduction (~80.40%), showing that the dye molecules were not only decoloured but also mineralized into simpler and less hazardous compounds.

## Conflict of interest

The authors declare no conflict of interest.

## Acknowledgment

The authors sincerely thank Kavayitri Bahinabai Chaudhari North Maharashtra University, Jalgaon for providing instrumental facilities.

## Supplementary Information

Supplementary information is available on the website https://nopr.niscpr.res.in/handle/123456789.

## References

1 Sun H, Qin P, Liang Y, Yang Y, Zhang J, Guo J, Hu X, Jiang Y, Zhou Y, Luo L & Wu Z, Sonochemically assisted the synthesis and catalytic application of bismuth-based photocatalyst: A mini review, *Ultrason Sonochem*, 100(2023) 106600.

2 Tiwari N, Chakrabortty S, Samal K, Moulick S, Mohapatra B G, Samanta S, Mohapatra P K, Sanjay K, Nayak J, Banerjee S & Tripathy S K, Photocatalytic degradation of malachite green using $TiO_2$ and ZnO impregnated on fecal sludge derived biochar, *J Taiwan Inst Chem Eng*, 145 (2023) 104800.

3 Elkady M F & Hassan H S, Photocatalytic degradation of malachite green dye from aqueous solution using environmentally compatible Ag/ZnO polymeric nanofibers, *Polymers*, 13 (2021) 2033.

4 Podasca V E & Damaceanu M D, Photopolymerized films with ZnO and doped ZnO particles used as efficient photocatalysts in malachite green dye decomposition, *Appl Sci*, 10 (2020) 1954.

5 Yadav R, Chundawat T S, Rawat P, Rao G K & Vaya D, Photocatalytic degradation of malachite green dye by ZnO and ZnO–β-cyclodextrin nanocomposite, *Bull Mater Sci*, 44 (2021)250.

6 Bhole D K, Puri R G, Meshram P D & Sirsam R S, Photocatalytic degradation of methyl orange using doped ZnO nanocatalyst, *J Indian Chem Soc*, 97 (2020) 440.

7 Giram D & Das A, Synthesis and characterization of Fe doped ZnO nanoparticles for the photocatalytic degradation of eriochrome black-t dye, *Indian J Chem Technol*, 31 (2024) 39.

8 Kabir R, Saifullah M A, Ahmed A Z, Masum S M & Molla M A, Synthesis of N-doped ZnO nanocomposites for sunlight photocatalytic degradation of textile dye pollutants, *J Compos Sci*, 4 (2020) 49.

9 Sanakousar F M, Vidyasagar C C, Jiménez-Pérez V M & Prakash K, Recent progress on visible-light-driven metal and non-metal doped ZnO nanostructures for photocatalytic degradation of organic pollutants, *Mater Sci Semicond Process*, 140 (2022) 106390.

10 Zheng A L T, Abdullah C A C, Chung E L T & Andou Y, Recent progress in visible light-doped ZnO photocatalyst for pollution control, *Int J Environ Sci Technol*, 20 (2022) 5753.

11 Suresh M & Sivasamy A, Fabrication of graphene nanosheets decorated by nitrogen-doped ZnO nanoparticles with enhanced visible photocatalytic activity for the degradation of methylene blue dye, *J Mol Liq*, 317 (2020) 114112.

12 Ou R, Zeng Z, Ning X, Zeng B & Wu C, Improved photocatalytic performance of N-doped ZnO/graphene/ZnO sandwich composites, *Appl Surf Sci*, 577 (2022) 151856.

13 Sun S, Chang X, Li X & Li Z, Synthesis of N-doped ZnO nanoparticles with improved photocatalytical activity, *Ceram Int*, 39 (2013) 5197.

14 Rajbongshi B M, Ramchiary A & Samdarshi S K, Influence of N-doping on photocatalytic activity of ZnO nanoparticles under visible light irradiation, *Mater Lett*, 134 (2014) 111.

15 Wu C, Zhang Y C & Huang Q, Solvothermal synthesis of N-doped ZnO microcrystals from commercial ZnO powder with visible-light-driven photocatalytic activity, *Mater Lett*, 119 (2014) 104.

16 Byzynski G, Melo C, Volanti D P, Ferrer M M, Gouveia A F, Ribeiro C, Andrés J & Longo E, The interplay between morphology and photocatalytic activity in ZnO and N-doped ZnO crystals, *Mater Des*, 120 (2017) 363.

17 Sudrajat H & Babel S, A novel visible light active N-doped ZnO for photocatalytic degradation of dyes, *J Water Process Eng*, 16 (2017) 309.

18 Oliveira J A, Nogueira A E, Gonçalves, M C P, Paris E C, Ribeiro C, Poirier G Y & Giraldi T R, Photoactivity of N-doped ZnO nanoparticles in oxidative and reductive reactions, *Appl Surf Sci*, 433 (2018) 879.

19 Prabakaran E & Pillay K, Synthesis of N-doped ZnO nanoparticles with cabbage morphology as a catalyst for the efficient photocatalytic degradation of methylene blue under uv and visible light, *RSC Adv*, 9 (2019)7509.

20 Giram D, Das A & Bhanvase B, Comparative study of ZnO-$TiO_2$ nanocomposites synthesized by ultrasound and conventional methods for the degradation of methylene blue dye, *Indian J Chem Technol*, 30 (2023) 693.

21 Adamou P, Harkou E, Hafeez S, Manos G, Villa A, Al-Salem S M, Constantinou A & Dimitratos N, Recent progress on sonochemical production for the synthesis of efficient photocatalysts and the impact of reactor design, *Ultrason Sonochem*, 100 (2023) 106610.

22 Vardikar H S, Bhanvase B A, Rathod A P & Sonawane S H, Sonochemical synthesis, characterization and sorption study of Kaolin-Chitosan-$TiO_2$ ternary nanocomposite: advantage over conventional method, *Mater Chem Phys*, 217 (2018) 457.

23 Raval N P, Shah P U & Shah N K, Malachite green "a cationic dye" and its removal from aqueous solution by adsorption, *App Water Sci*, 7 (2017) 3407.

24 Giram D, Shrivastava T & Das A, Ultrasound assisted synthesis of Fe doped $TiO_2$ nanoparticles for enhanced photocatalytic degradation of ciprofloxacin, *J Sci Ind Res*, 83 (2024) 711.

25 Pigosso T, Melo B A A, Evangelista L L, Gómez González, S Y & Binder C, Rapid synthesis of in situ nitrogen-doped ZnO nanoparticles for visible-light-driven photocatalytic removal of emerging contaminants, *Mater Today Chem*, 33 (2023) 101753.

26 Hop D T B, Tuan T Q, Quang N V, Tu N, Tien H L, Tran M T, Vinh T Q, Tu N C, Bach T N, Dao V D & Huong P T L, Enhanced visible-light photocatalytic degradation efficiency of $Ce^{3+}$-doped ZnO nanoparticles synthesized by sol-gel method, *Ceram Int*, 50 (2024) 17338.

27 Rangel R, Cedeño V, Ramos-Corona A, Gutiérrez R, Alvarado-Gil J J, Ares O, Bartolo-Pérez P & Quintana P, Tailoring surface and photocatalytic properties of ZnO and nitrogen-doped ZnO nanostructures using microwave-assisted facile hydrothermal synthesis, *Appl Phys A*, 123 (2017) 552.

28 Devi V S S, Balraj B, Siva C & Amuthameena S, Synthesis of nitrogen-doped zinc oxide nanomaterials for hydrogen gas sensing applications, *J Mater Sci Mater Electron*, 34 (2023) 1905.

29 Devi K N, Devi S A, Singh W J & Singh K J, Nickel doped zinc oxide with improved photocatalytic activity for malachite green dye degradation and parameters affecting the degradation, *J Mater Sci Mater Electron*, 32 (2023) 8733.

30 Shah P, Unnarkat A, Patel F, Shah M & Shah P A, Comprehensive review on spinel based novel catalysts for visible light assisted dye degradation, *Process Saf Environ Prot*, 161 (2022) 703.

31 Satdeve N S, Ugwekar R P & Bhanvase B A, Ultrasoundassisted preparation and characterization of Ag supported on ZnO nanoparticles for visible light degradation of methylene blue dye, *J Mol Liq*, 291 (2019) 111313.

32 Fulzele N N, Bhanvase B A & Pandharipande S L, Sonochemically prepared rGO/$Ag_3PO_4$/$CeO_2$ nanocomposite photocatalyst for effective visible light photocatalytic degradation of methylene dye and its prediction with ann modeling, *Mater Chem Phys*, 292 (2022) 126809.

33 Kumari V, Mittal A, Jindal J, Yadav S & Kumar N, S-, N-and C-Doped ZnO as Semiconductor Photocatalysts : A Review, *Front Mater Sci*, 13 (2019) 1.